

# Stability Analysis of Four $f(Q)$ Gravity Models : A Cosmological Review in the Background of Bianchi-I Anisotropy

*Subhajit Pal*<sup>\*1</sup>, *Atanu Mukherjee*<sup>\*\*2</sup>, *Ritabrata Biswas*<sup>\*\*3</sup> and *Farook Rahaman*<sup>\* 4</sup>

*\*Department of Mathematics, Jadavpur University, Kolkata-32, India*

*\*\*Department of Mathematics, The University of Burdwan, Burdwan-713104, India*

## Abstract

With the non-metricity scalar  $Q$  as the functional argument, several  $f(Q)$  gravity models is found to be proposed which are perfectly able to mimic the late time accelerated expansion as pointed out by the type Ia supernovae observations. Temperature fluctuation differences for two celestial hemispheres, Hubble tension, voids, dipole modulation, anisotropic inflation etc motivates us to think beyond the  $\Lambda$ CDM model and cosmological principle. Bianchi-I model portrays anisotropic universe imposing shear.  $f(Q)$  model also enables us to produce early inflation to late deSitter universe without the requirement of  $\Lambda$ CDM. Embarrassment regarding fine tuning or coincidences can be avoided alongwith. So, this article finds different stationary points of cosmic evolution with  $f(Q)$  models habilitating in Bianchi-I anisotropic universe. Depending on models' nature, fixed points with different categories are found. Perturbations are followed wherever are applicable. While pursuing cosmological implications towards these fixed points, some are found to be formed only for the consideration of  $f(Q)$  gravity and Bianchi-I both. Besides different prediction towards early inflation to late time expansion which are available in existing literature of dynamical system studies, occurances of ultra slow roll inflation is predicted. For particular  $f(Q)$  model, shear is predicted to decay leaving behind a constant valued residue. This models a universe that gradually turns more homogeneous. In some other models, depending on initial conditions, a final isotropic leftover is marked as the future fate of anisotropic world. More than one stable points are marked for special cases and are cosmologically interpreted.

Keywords : Anisotropic universe, Dynamical system, Center manifold theory

PACS No.: 98.80.Cq, 04.20.Jb, 98.80.Jp, 98.30Cq, 98.80Cw, 04.50.Kd, 05.40.-a

## 1 Introduction

As explained by the cosmological principle, our universe is postulated to be both homogeneous and isotropic on a large scale. This generates a framework described by the Friedmann–Lemaître–Robertson–Walker (FLRW) geometry. In recent years, observations of the universe's expansion rate and structure at early

---

<sup>1</sup>subhajitpal968@gmail.com ; Orchid : 0009 – 0002 – 2431 – 1375

<sup>2</sup>atanu2002mukherjee@gmail.com ; Orchid : 0009 – 0003 – 3230 – 0059

<sup>3</sup>biswas.ritabrata@gmail.com ; Orchid : 0000 – 0003 – 3086 – 892X

<sup>4</sup>farookrahaman@gmail.com ; Orchid : 0000 – 0003 – 0594 – 4783

times (e.g., from the Cosmic Microwave Background (CMB)) and late times (e.g., from supernovae, baryon acoustic oscillations (BAO) and galaxy surveys) have shown inconsistencies or “tensions”. One conspicuous example is the Hubble tension. Early universe measurements from the Planck satellite, assuming standard cosmological model that describes the universe, incorporating a cosmological constant (represented by the Greek letter lambda,  $\Lambda$ ) associated with dark energy (DE), and cold dark matter (CDM) –  $\Lambda$ CDM, speculate the present day value of Hubble parameter,  $H_0 \approx 67.4 \pm 0.5 \text{ km s}^{-1}/\text{Mpc}$  [1]. On the contrary, from the late universe measurements, predicted from type Ia supernovae observation, the project Supernova,  $H_0$ , for the Equation of State (SH0ES collaboration), the value of  $H_0$  is found to be  $\approx 73.2 \pm 1.3 \text{ km s}^{-1}/\text{Mpc}$  [2]. The discrepancy between these two measurements is the most prominent tension in the context of the Hubble tension. These tensions suggest that the standard  $\Lambda$ CDM model which assumes general relativity (GR) and the cosmological principle, might be incomplete or there must be a missing key of physics.

Alternative scenario thus required involves either modified gravity theories or relaxation on the cosmological principle considering universes that are not perfectly homogeneous or isotropic, especially in the early stages. This leads to different models like Bianchi cosmologies (anisotropic but homogeneous) and Lemaitre–Tolman–Bondi (LTB) models (inhomogeneous).

Observationally, anisotropies and inhomogeneities are supported from the cosmic microwave background (CMB) radiation which is the relic radiation from the surface of last scattering about 380,000 years after the Big Bang when photons were decoupled from matter[3]. It is followed that the quadrupole ( $l = 2$ ) moment of the CMB power spectrum is lower than that predicted by  $\Lambda$ CDM. Its statistical significance alone is not strong ( $\sim 2 - 2.5\sigma$ ) but it is a part of a set of correlated anomalies[4]. Wilkinson Microwave Anisotropy Probe (WMAP) followed that the amplitude of temperature fluctuations appears stronger in one hemisphere of the sky compared to the other[5]. A large, unusually cold region, centered near galactic coordinates  $(l, b) \approx (209^\circ, -57^\circ)$ , was detected in WMAP and confirmed by Planck [6]. These dipole modulation, anisotropic inflation, void etc point towards anisotropies.

Now, we will consider the metric-affine geometry where the metric  $g_{\mu\nu}$  and the affine connection  $\Gamma_{\mu\nu}^\lambda$  are independent. If we impose both the curvature and the torsion to vanish, i.e.,  $R_{\mu\nu\rho}^\lambda = T_{\mu\nu}^\lambda = 0$ , the non-metricity is only allowed not to vanish identically. The non-metricity tensor takes the form :

$$Q_{\lambda\mu\nu} = \nabla_\lambda g_{\mu\nu} \neq 0 \quad . \quad (1)$$

We define two traces :

$$Q_\lambda = Q_{\lambda\mu}^\mu \quad \text{and} \quad \bar{Q}_\lambda = Q_{\mu\lambda}^\mu \quad . \quad (2)$$

The superpotential tensor  $P_{\mu\nu}^\lambda$  is given by,

$$P_{\mu\nu}^\lambda = \frac{1}{4} \left( -Q_{\mu\nu}^\lambda + 2Q_{(\mu\nu)}^\lambda - Q^\lambda g_{\mu\nu} - \bar{Q}^\lambda g_{\mu\nu} \right) \quad . \quad (3)$$

This has a similar role to the Einstein’s tensor in GR.

Using the superpotential tensor, we can form a scalar in connections with the non-metricity tensor given by,

$$Q = -g^{\mu\nu} \left( P_{\mu\nu}^\lambda Q_\lambda^{\mu\nu} \right) \quad . \quad (4)$$

This non-metricity scalar  $Q$  plays almost a similar role as the Ricci scalar  $R$  plays in GR.

The action of  $f(Q)$  gravity is given by,

$$\mathcal{S} = \int \sqrt{-g} \left[ \frac{1}{2} f(Q) + \mathcal{L}_m \right] d^4x \quad , \quad (5)$$

where  $f(Q)$  is the arbitrary function of the non-metricity scalar  $Q$  and  $\mathcal{L}_m$  is the matter Lagrangian.

Varying the action with respect to the metric  $g_{\mu\nu}$ , equation (5) gives,

$$\frac{2}{\sqrt{-g}} \nabla_\lambda \left( \sqrt{-g} f_Q P_{\mu\nu}^\lambda \right) + \frac{1}{2} g_{\mu\nu} f(Q) + f_Q \left( P_{\mu\lambda\rho} Q_\nu^{\lambda\rho} - 2Q_{\lambda\rho\mu} P_\nu^{\lambda\rho} \right) = T_{\mu\nu} \quad , \quad (6)$$

where  $f_Q \equiv \frac{d}{dQ}f(Q)$  and  $T_{\mu\nu}$  is the energy-momentum tensor.

The Bianchi-I metric is the simplest anisotropic generalization of the flat FLRW metric. This describes a spatially homogeneous but anisotropic universe where expansion can vary in different spatial directions. The metric in comoving coordinates  $(t, x, y, z)$  is given as

$$ds^2 = -dt^2 + \sum_{i=0}^3 a_i^2(t)(dx^i)^2 \quad , \quad (7)$$

where  $a_1^2(t)$ ,  $a_2^2(t)$  and  $a_3^2(t)$  respectively are the directional scale factors describing how distances expand respectively along the  $x$ ,  $y$  and  $z$  axes. There is no spatial dependence in the metric function. Only a time dependence is followed. This means every point in space is geometrically identical at a given time. The scenario turns homogeneous as a result. However, the inequality of  $a_1(t)$ ,  $a_2(t)$  and  $a_3(t)$  indicates different rates of expansion or contraction in different directions.

For this current situation, in anisotropic Bianchi-I space-time metric (7), the directional Hubble parameters are given by,  $H_i = \frac{\dot{a}_i}{a_i}$ ,  $\cdot \equiv \frac{d}{dt}$ . Hubble parameter can be defined by the arithmetic mean of these three directions' Hubble parameters, given by,

$$H_{AM}(t) = \frac{1}{3} [H_1 + H_2 + H_3] \quad . \quad (8)$$

We also denote the scale factor  $a_{GM}(t)$  as the geometric mean of the directional scale factors, given by,

$$a_{GM}(t) = [a_1(t)a_2(t)a_3(t)]^{\frac{1}{3}} \quad . \quad (9)$$

Now, we can use the parametrisation,

$$a_i(t) = a_{GM}(t)e^{\beta_i(t)} \quad . \quad (10)$$

Then calculating we get,

$$H_i = H + \beta_i \quad , \quad \beta_1 + \beta_2 + \beta_3 = 0 \quad . \quad (11)$$

The space-time metric admits three isometries associated with the vector fields  $\partial_x$ ,  $\partial_y$  and  $\partial_z$  respectively.

The Bianchi-I geometry, given in Cartesian coordinates, possesses the nonzero components of the three Christoffel connections as,

$$\begin{aligned} \Gamma_1 & : \Gamma_{tt}^t = \gamma(t) \quad , \\ \Gamma_2 & : \Gamma_{tt}^t = \gamma(t) + \frac{\dot{\gamma}(t)}{\gamma(t)} \quad , \quad \Gamma_{tx}^x = \Gamma_{ty}^y \Gamma_{yz}^z = \gamma(t) \quad \text{and} \\ \Gamma_3 & : \Gamma_{tt}^t = -\frac{\dot{\gamma}(t)}{\gamma(t)} \quad , \quad \Gamma_{tx}^t = \Gamma_{ty}^t \Gamma_{yz}^t = -\gamma(t) \quad , \end{aligned}$$

where the function  $\gamma$  introduces dynamic degrees of freedom in the field equation.

The non-metricity scalar  $Q$ , derived from the connection of  $\Gamma_1$  is obtained as,

$$Q = 2 \sum H_i H_j = 6H^2 - \sigma^2 \quad , \quad \text{where} \quad (12)$$

$$\sigma^2 = -2 \sum \dot{\beta}_i \dot{\beta}_j = \sum \dot{\beta}^2 \quad . \quad (13)$$

Note that  $\sigma = 0$  implies  $\sum \dot{\beta}^2 = 0$  which means the universe is an isotropic FLRW.

The anisotropic fluid is defined as,

$$T_{\mu}^{\nu} = \text{diag}(-\rho, P_1, P_2, P_3) = \text{diag}(-\rho, \omega_1\rho, \omega_2\rho, \omega_3\rho) \quad , \quad (14)$$

where  $\rho$  denotes the energy density of the fluid,  $P_1$ ,  $P_2$  and  $P_3$  are the pressure along the three orthogonal directions. The directional equation of state (EoS) parameters are  $\omega_1$ ,  $\omega_2$  and  $\omega_3$ . Then the average EoS parameter  $\omega$  is given by,

$$\omega = \frac{1}{3}(\omega_1 + \omega_2 + \omega_3) \quad , \quad (15)$$

and the deviations  $\mu_i$  can be calculated from the average EoS as,

$$\mu_i = \omega_i - \omega \quad , \quad \text{or, } \omega_i = \omega + \mu_i \quad , \quad \text{for } i = 1, 2, 3 \quad . \quad (16)$$

However, for the isotropic fluid,  $P_1 = P_2 = P_3 = P = \omega\rho$ .

Now, the modified Friedmann and the Raychaudhuri equations for our case can be expressed as (for simplification, writing  $H_{AM}$  as  $H$  and  $a_{GM}$  as  $a$ ),

$$3H^2 - \sigma^2 = \frac{\kappa}{f_Q} \left[ \rho - \frac{3H^2 f_Q}{\kappa} - \frac{f}{2\kappa} \right] \quad \text{and} \quad (17)$$

$$-(2\dot{H} + 3H^2) - \frac{\sigma^2}{2} = \frac{\kappa}{f_Q} \left[ \omega_\rho + \frac{f}{2\kappa} + \frac{2H\dot{f}_Q}{\kappa} - \frac{Qf_Q}{2\kappa} \right] \quad . \quad (18)$$

The equations (17) and (18) can be simplified, taking into account the expression for  $Q$  from (12), as

$$3H^2 - \frac{\sigma^2}{2} = \frac{\kappa}{f_Q} \left[ \rho - \frac{f}{2\kappa} \right] \quad \text{and} \quad (19)$$

$$-(2\dot{H} + 3H^2) - \frac{\sigma^2}{2} = \frac{\kappa}{f_Q} \left[ \omega_\rho + \frac{f}{2\kappa} + \frac{2H\dot{f}_Q}{\kappa} \right] \quad , \quad \text{where} \quad (20)$$

$$\dot{\sigma} = -\sigma \left( \frac{\dot{f}_Q}{f_Q} + 3H \right) \quad . \quad (21)$$

The last equation is known as an anisotropic evolution equation. Integrating we have,

$$\sigma \sim \frac{1}{a^3 f_Q} \quad . \quad (22)$$

Locally Rotationally Symmetric (LRS) Bianchi type-I universe within the framework of a novel modified  $f(Q)$  gravity theory is studied in the article [7]. In this theory, gravitational interactions are chosen to be governed by the non-metricity tensor  $Q$ , under the assumption of vanishing curvature and torsion. Fixed points are found to signify quintessence-like DE cosmological scenario as well as the phantom DE cosmological model. Authors of the article [8] focused on solutions defined in the coincident gauge where the authors identify Kasner-like solutions that is built upon the original Kasner relations. Interestingly, the characteristics of the indices for these exact solutions remain consistent which suggests that they exhibit similar behavior to that of the Kasner universe. On the other hand, in the same work, other two sets of field equations defined by connections in the non-coincident gauge along with self-similar solutions are found that do not adhere to the Kasner-like constraint equations. This observation implies that the chaotic behavior typically seen in the Mixmaster universe, especially near singularities, which may not be present in the context of symmetric teleparallel  $f(Q)$ -gravity.

General forms of homogeneous and isotropic symmetric teleparallel geometries are identified in the article [9]. One solution with spatial curvature (where  $k \neq 0$ ) is followed to meet the symmetry conditions. Three distinct branches of spatially flat geometries (where  $k = 0$ ) are noted, each of which can be derived as a specific limit from the common spatially curved case as  $k$  approaches zero. Each of these branches is characterized by two scalar functions of time, viz., the cosmological scale factor  $a$  in the metric and another scalar  $K$  that describes the symmetric teleparallel connection. A third function, the lapse  $N$ , can

be adjusted through a choice of time coordinate. For each branch, the coincident gauge was found where the coefficients of the symmetric teleparallel connection vanish. Only one of these branches retains the Friedmann-Lemaître-Robertson-Walker (FLRW) form in the coincident gauge.

Cosmological dynamical systems that emerge from various modified theories of gravity are explored model independently in the article [10] by concentrating on theories characterized by second-order field equations such as those in  $f(G)$ ,  $f(T)$ , and  $f(Q)$  gravity theories. For instance, in  $f(R)$  gravity, the Ricci scalar contains terms that are proportional to both  $H$  and  $\dot{H}$ , which means that the variables chosen are not sufficient to fully close the system. The system will always be closed once a function  $f$  is specified, because any function of  $G$ ,  $T$  or  $Q$  can be expressed as a function of  $H$ . This flexibility also extends to non-minimal couplings of matter, as long as the equations remain of second order.

The article [11] analyzes  $f(Q)$  gravity in spatially flat FLRW space-time using dynamical systems, revealing stable deSitter solutions and unstable matter-dominated phases, highlighting the role of non-vanishing affine connections. Authors of the articles [12, 13, 14] have investigated a non-flat FLRW universe, finding curvature driven inflationary points and solutions alleviating the coincidence problem. The research of [14] explores Bianchi-I cosmologies in  $f(Q)$  gravity using the 1 + 3 covariant formalism and dynamical system analysis. The article [7] analyses the Locally Rotational Symmetric (LRS) Bianchi-I model in  $f(Q)$  gravity. Also it links the saddle and stable critical points to quintessence and phantom DE scenarios. Also, finding the heteroclinic connections between radiation, matter and dark energy dominated phases are explored in [15].

The modified gravity can contribute to explaining anomalies in Cosmic Microwave Background(CMB) like the quadrupole suppression or axis of evil. Study of  $f(Q)$  gravity offers new candidates for dark energy. This theory may avoid fine-tuning problems of  $\Lambda$ CDM. Bianchi-I background enables detailed perturbation analysis in anisotropic settings which inform  $N$ -body simulations in non-standard cosmologies. This study of  $f(Q)$  can investigate how non-metricity drives inflation in anisotropic setups. It can fit anisotropic models with SNe Ia, BAO, CMB.

Dynamical system studies for  $f(Q)$  gravity in the background of the Bianchi-I type anisotropic universe is important for theoretical, observational and cosmological reasons. This model is expected to probe the early universe anisotropies good. CMB observations suggest the possibility of small anisotropies or preferred directions. Investigating  $f(Q)$  gravity in this context helps us to test whether geometric generalizations like symmetric teleparallelism can naturally resolve or damp anisotropies. A viable modified gravity theory should reproduce isotropy at late times and allow anisotropy at early times. Dynamical systems help to test this evolution. GR tends to isotropize the universe at late times (Wald's theorem), but it is not guaranteed in modified theories.  $f(Q)$  gravity modifies the connection based description of gravity. The dynamical system analysis mass reveal whether  $f(Q)$  models allow natural isotropization. A dynamical system approach may help classifying models according to late-time cosmic acceleration, matter dominated era, stability and robustness analysis etc. [16, 17, 18]

In the next section, we will construct general dynamical system equations for  $f(Q)$  gravity in Bianchi-I cosmology. In section 3, we will analyse dynamical systems for different  $f(Q)$  models. Phase portraits will be thoroughly checked and different equilibrium points will be physically interpreted. Finally, in section 4, a brief discussion of the work will be incorporated.

## 2 Dynamical Systems for Some $f(Q)$ Candidates in Bianchi-I Cosmology

Define the dimensionless variables as,

$$x = \frac{\kappa\rho}{6f_Q H^2}, \quad y = -\frac{f}{12f_Q H^2} \quad \text{and} \quad z = \frac{\sigma^2}{6H^2}. \quad (23)$$

Constrained by the relation (19)

$$x + y + z = 1 \quad . \quad (24)$$

Now, the dynamical system equations can be constructed by taking the derivatives of the dimensionless variables  $x$ ,  $y$  and  $z$  with respect to the variable  $N = \ln a$ , given as,

$$x' = -3x(1 + \omega) + 6x \left\{ \frac{(y - 1 - x\omega)(1 + \Gamma - \Gamma z - 2z)}{(\Gamma + 2)(z - 1)} \right\} - \frac{6xz}{(\Gamma + 2)(z - 1)} \quad , \quad (25)$$

$$y' = 3\Gamma \left( \frac{z + y - 1 - x\omega}{\Gamma + 2} \right) + 6y \left[ \frac{(y - 1 - x\omega)(1 + \Gamma - \Gamma z - 2z)}{(\Gamma + 2)(z - 1)} \right] - \frac{6yz}{(\Gamma + 2)(z - 1)} \quad \text{and} \quad (26)$$

$$z' = 6z(x\omega - y) \quad , \quad (27)$$

where “( ’)” denotes the derivative w.r.to  $N = \ln a$ . Then we have the auxiliary quantity  $\Gamma = \Gamma(Q)$  as,

$$\Gamma = \frac{f_Q}{Q f_{QQ}} \quad . \quad (28)$$

Now, by using (21), we have,

$$\frac{\dot{H}}{H^2} = 3 \left\{ \frac{(2z + z\Gamma - \Gamma)(y - 1 - x\omega) + 2z}{(\Gamma + 2)(z - 1)} \right\} \quad . \quad (29)$$

Eliminating the variable  $y$ , the above dynamical system will be reduced to,

$$x' = -3x(1 + \omega) + 6x(x + z + x\omega) + 6x \frac{x + x\omega}{(\Gamma + 2)(z - 1)} \quad \text{and} \quad (30)$$

$$z' = 6zx(1 + \omega) + 6z^2 - 6z \quad , \quad (31)$$

while the equation (29) is reduced to,

$$\frac{\dot{H}}{H^2} = 3 \left\{ \frac{(2z + z\Gamma - \Gamma)(-z - x - x\omega) + 2z}{(\Gamma + 2)(z - 1)} \right\} \quad . \quad (32)$$

The equation (32) helps us to determine the cosmic evaluation for a particular fixed point.

For a  $f(Q)$  gravity model, we need to express  $Q$  and hence  $\Gamma(Q)$  in terms of the dynamical variables  $x$  and  $z$ . Now from the equations (12) and (23), we can construct the value of  $Q$  as,

$$\frac{Q f_Q}{f} = \frac{(1 - z)}{2y} \quad . \quad (33)$$

By using the expression of the equation (24), one can derive,

$$\frac{Q f_Q}{f} = \frac{(1 - z)}{2(1 - x - z)} \quad . \quad (34)$$

Thus, we can say, from the above equations, that  $Q = Q(x, z)$ . By using the expression of  $\Gamma(Q)$ , one can obtain an autonomous dynamical system for the connection  $\Gamma_1$  for the Bianchi-I cosmology with an isotropic fluid in the modified gravity or  $f(Q)$  gravity.

In the next section, phase portrait analysis of individual  $f(Q)$  models chosen will be performed.

### 3 Stability Analysis for Different $f(Q)$ Gravity Candidates

In this section, we calculate the stability of the different  $f(Q)$  gravity models for the Bianchi-I in the connection  $\Gamma_1$ . To perform this analysis in the presence of the matter component and will plot the phase portraits for every model.

### 3.1 Model I : $f(Q) = mQ^n$

The model  $f(Q) = mQ^n$  is known as a power law model with the parameters  $m$  which sets the strength of the gravitational computing and  $n$  which determines how non-linearly the gravity theory depends on the scalar  $Q$ . At  $n = 1$ , this model reduces to  $f(Q) = mQ$  which is equivalent to GR if  $m = 1$ . For specific powers  $n > 1$ , this model can mimic inflationary potentials without incorporating scalar fields like the inflation in standard models [19]. With  $n = 2$ , Starobinsky inflation in  $f(R) = R + R^2$  is mimicked which is found by Planck CMB data. The second order field equations make it easier to avoid instabilities common in higher derivative inflationary model. This model also modifies the tensor to scalar ratio  $r$ , affecting gravitational wave signals from inflation [20]. For  $0 < n < 1$ , the modifications to gravity weakens gravitational attraction at large scales, mimicking a repulsive force. This is indicative towards the late time cosmic acceleration. The model allows the Hubble parameter to evolve in a way consistent with supernovae type Ia, BAO and CMB data [21]. In general, a gravity model affects the generation and propagation, amplitude decay, polarization of gravitational waves(GWs). After the GW170817 event [22] confirmed GWs travel at light's speed,  $f(Q) = mQ^n$  gravity got a huge support as this too predicts GW's speed to be equal to that of light in vacuum.  $f(Q) = mQ^n$  modifies the Poisson equation and growth equation for matter density perturbation given by  $\ddot{\delta} + 2h\dot{\delta} - 4\pi G_{eff}\rho\delta = 0$ , where  $\delta \equiv \frac{\delta\rho}{\rho}$  is the matter density contrast and  $G_{eff}$  is the effective gravitational constant which can differ from Newton's  $G_N$  in modified gravity theories like  $f(Q)$  gravity. This affects the growth rate  $f = \frac{d\ln\delta}{d\ln a}$  and the matter power spectrum[20]. This predicts towards different growth and structure formation histories compared to  $\Lambda$ CDM which is testable via redshift-space distortion, gravity clustering weak lensing surveys etc[20].

Now, the  $Q$  derivatives of the model-I can be obtained as,

$$f_Q = mnQ^{n-1} \quad \text{and} \quad (35)$$

$$f_{QQ} = mn(n-1)Q^{n-2} \quad . \quad (36)$$

Setting the values of  $f_Q$  for the specific model-I into the equation (34), we obtain the additional constraints

$$z = \frac{2n(x-1)+1}{1-2n} = 1 - \frac{2nx}{2n-1} \quad . \quad (37)$$

Substituting equations (35) and (36) in equation (28), we obtain,

$$\Gamma = \frac{1}{n-1} \quad . \quad (38)$$

Substituting the expression of  $\Gamma$  from (38), we get the dynamical system as,

$$x' = 3x \left( -1 - \omega + \frac{2x(1+\omega)}{(2 + \frac{1}{n-1})(-1+z)} + 2(x+z+x\omega) \right) \quad \text{and} \quad (39)$$

$$z' = 6z(x\omega + x + z - 1) \quad . \quad (40)$$

For this particular model,  $f(Q) = mQ^n$ , equation (32) gives,

$$\frac{\dot{H}}{H^2} = \frac{3z \{-2n(z-1) + z - 1\} - 3x(\omega+1) \{(2n-1)z - 1\}}{(2n-1)(z-1)} \quad . \quad (41)$$

In table 1, we note all the categories of critical points. Fig 1a – 1d are  $z$  vs  $x$  phase diagrams for different values of  $n$  and  $\omega$ . Red, green and blue dots do signify stable, saddle and unstable points respectively.

Hyperbolic stable points ensure the universe always ends up in the same state, regardless of tiny differences in the past. This is important for explaining why today's universe is so isotropic and accelerating. As the hyperbolic stable point lies on the axis, the universe naturally evolves to an isotropic state. Again the

Crit. Point	Existence	Eigenvalues	Type of crit. point	Stability	Cosmology
$x \rightarrow 0$	$\forall \omega$	$-6$ and $-6$	Hyperbolic ( $\forall \omega$ )	Stable node	$a(t) = a_0 e^{H_0 t}$ (i.e., deSitter)
$x \rightarrow \frac{2n-1}{2n}$	$n \neq 0,$ $\forall \omega$	$\frac{3}{n} \{(2n-1)\omega - 1\}$ and $3(\omega + 1)$	Hyperbolic ( $\omega \neq -1, \frac{1}{2n-1}$ )	Stable node for ( $\omega < -1$ ) Saddle point for ( $\omega > -1, \omega < \frac{1}{2n-1}$ ) Unstable node for ( $\omega > -1, \omega > \frac{1}{2n-1}$ )	$a(t) \propto t^{-\frac{2n}{3(\omega+1)}}$
			Non-hyperbolic ( $\omega = -1, \frac{1}{2n-1}$ )	Central manifold for ( $n = -1, \frac{1}{2n-1}$ )	

Table 1: Critical points with existence conditions, eigen values, type of critical points, stability and cosmology pattern for model-I:  $f(Q) = mQ^n$ .

hyperbolic stable point corresponds to  $x = 0$ , i.e.,  $\dot{H} = 0$ , it gives constant Hubble rate, i.e., accelerating expansion like DE. Only certain values of  $n$  in  $f(Q) = mQ^n$  give realistic cosmic evolution with a hyperbolic stable attractor. Now to explain hyperbolic saddle, we notice that the saddle points with non zero shear ( $E^2 \neq 0$ ) are often formed in Bianchi-I models. These saddle points describe a universe that starts anisotropic but gradually evolves towards isotropy. Physically, this supports the idea that anisotropies decay over time due to the dynamics of  $f(Q)$  gravity.

Saddle points allow the universe to pass through realistic intermediate phases, like matter dominated phase (galaxy formation) or radiation dominance (CMB decoupling). This makes  $f(Q) = mQ^n$  gravity cosmologically viable, as it reproduces necessary eras of standard cosmology before reaching a late time attractor (accelerated expansion). In Bianchi-I cosmology, if a saddle point has non zero anisotropy, the system may start near this anisotropic state and then exits toward an isotropic attractor [23].

A hyperbolic unstable point is a natural candidate for the early universe. This represents a Big Bang like state (high curvature  $Q$ , large  $H$ ). Universe emerges near this state and then evolves away deterministically. Since it is hyperbolic and structurally stable, small perturbations would not change the qualitative behavior. Again Bianchi-I type early universe can be predicted which evolves quickly away, often into a matter saddle point and finally into a deSitter attraction. No fine tuning even is needed as the unstable node or foci repels trajectories generally and hence a wide range of initial conditions evolve naturally from this early phase [23].

Figure 1c spots a centre however. This points towards an oscillatory cosmology or a bouncing universe. Also, in a Bianchi-I geometry with shear, centres may correspond to oscillations in anisotropy. The shear variables oscillate around a mean, while the universe may slowed expand or remains bounded. These cycles can resemble mixmaster-like dynamics or approaches very slowly towards a stable deSitter or be chaotic but bounded states [24].

Introducing scalar perturbation to the metric and matter fields, we find

$$ds^2 = -(1 + 2\Phi)dt^2 + a_i^2(1 - 2\psi)dx^i dx^i \quad , \quad (42)$$

$$\rho = \bar{\rho} + \delta\rho \quad \text{and} \quad p = \bar{p} + \delta p \quad , \quad (43)$$

assuming  $\psi_1 = \psi_2 = \psi_3 = \psi$  (isotropic perturbations), the perturbed field equations are studied : Time-time perturbation for this model is given by,

$$6mn(2n-1)H^2(\dot{\psi} + H\phi) + mn(n-1)Q^{n-2}\delta Q = \delta\rho \quad \text{and} \quad (44)$$

space-space perturbation takes the form of,

$$2mnQ^{n-1}(\dot{\psi} + H\phi) + mn(n-1)Q^{n-2}(\dot{Q}\psi + Q\dot{\psi}) = -a^2\delta p \quad , \quad (45)$$

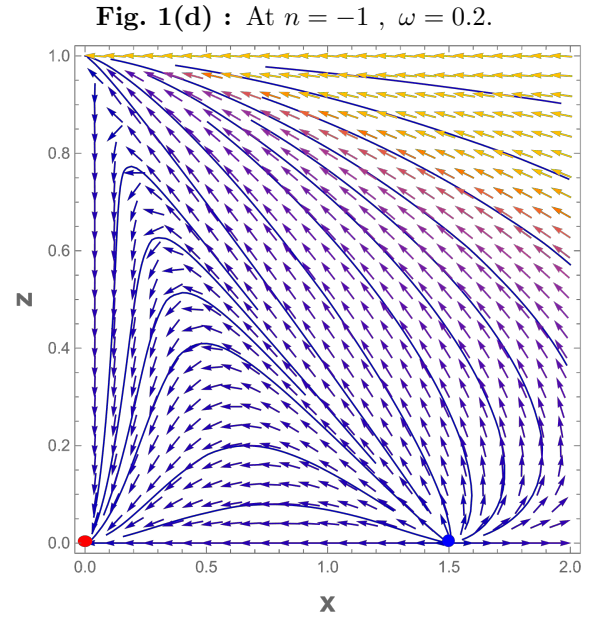
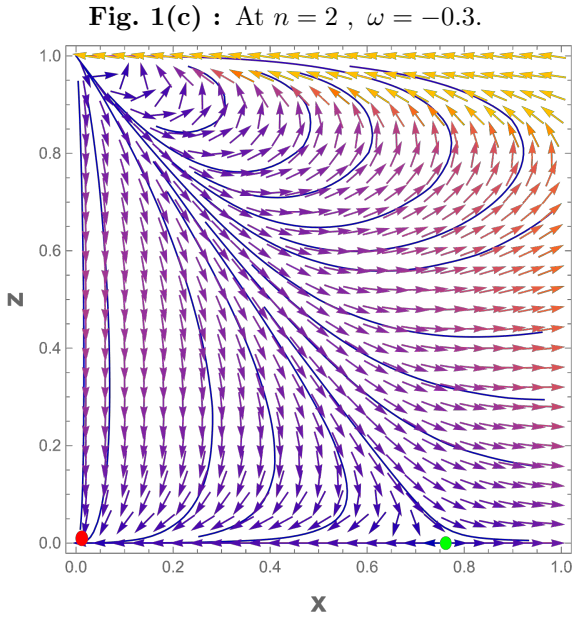
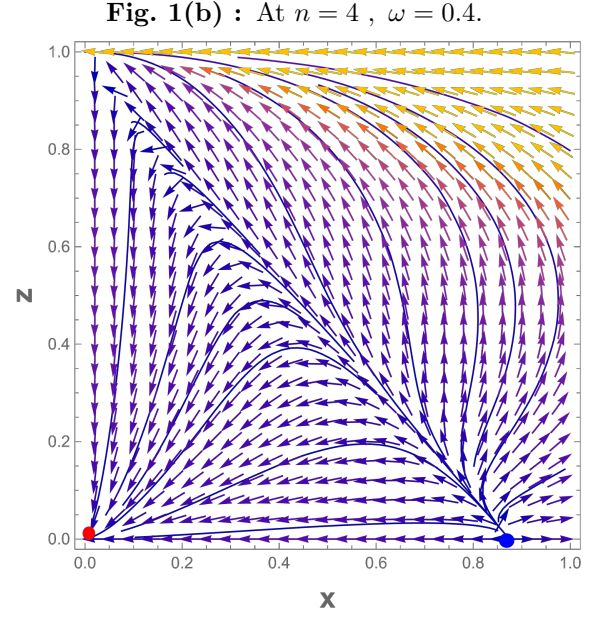
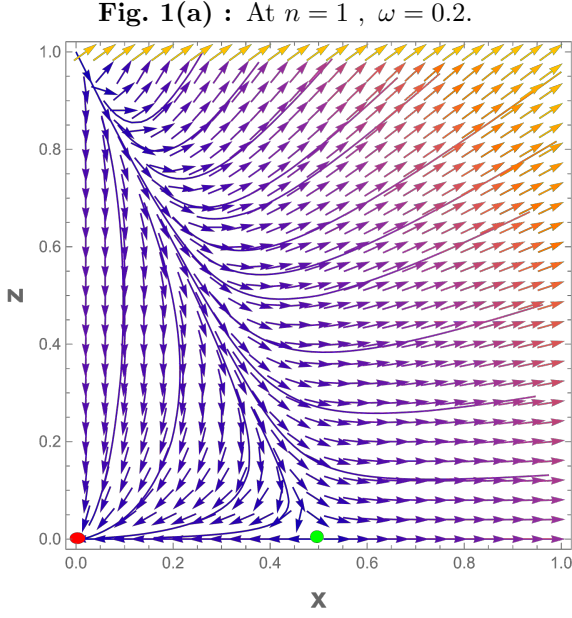


Figure 1: Figure (a) – (d) are  $z$  vs  $x$  phase diagrams for the model  $f(Q) = mQ^n$  in Bianchi I cosmology at different values of  $n$  and  $\omega$ . A red dot indicates a stable point, a green dot indicates a saddle point and a blue dot indicates an unstable point.

where the non-metricity perturbation  $\delta Q$  is given by,

$$\delta Q = 12H(\dot{\psi} + H\phi) \quad . \quad (46)$$

For the stability, sound speed squared  $C_s^2 = \frac{\delta p}{\delta \rho}$  must be real and positive. For the model  $f(Q) = mQ^n$ , the conditions are,

$$C_s^2 = \frac{2n-1}{3n-1} \quad \text{and} \quad mnQ^{n-1} > 0. \quad (47)$$

Thus for  $n > \frac{1}{2}$ ,  $c_s^2 > 0$  and  $m > 0$ , the no-ghost condition holds if  $Q > 0$ .

$$\ddot{h}_{ij} + \left( 3H + (n-1)\frac{\dot{Q}}{Q} \right) \dot{h}_{ij} + \frac{k^2}{a^2} h_{ij} = 0 \quad . \quad (48)$$

While working with the tensor perturbation, the tensor modes propagate with the speed :

$$C_T^2 = \frac{f_Q}{f_Q + 2Qf_{QQ}} = \frac{1}{2n-1} \quad . \quad (49)$$

In equation of  $x'$ , we can substitute the value of  $z$  and obtain

$$x' = \frac{3\{1 + 2n(x-1)\}x\{(2n-1)\omega - 1\}}{n(2n-1)} \quad \text{and} \quad (50)$$

in equation of  $z'$ , substituting the value of  $x$ , we get,

$$z' = -\frac{3}{n}(z-1)z\{(2n-1)\omega - 1\} \quad [\text{by incorporating the value of } z] \quad (51)$$

Linearizing around  $x = 0$ , we set  $x = \delta x$  and obtain,

$$\frac{d(\delta x)}{dN} \approx \frac{3(1-2n)\{(2n-1)\omega - 1\}\delta x}{n(2n-1)} = -\frac{3}{n}\{(2n-1)\omega - 1\}\delta x \quad (52)$$

$$\Rightarrow \delta x \sim \exp \left\{ -\frac{3}{n}\{(2n-1)\omega - 1\}N \right\} \quad (53)$$

Similarly, linearizing around  $z = 0$ , we set  $z = \delta z$  to follow that Then,

$$\frac{d(\delta z)}{dN} \approx \frac{3}{n}\{(2n-1)\omega - 1\}\delta z \quad (54)$$

$$\Rightarrow \delta z \sim \exp \left\{ \frac{3}{n}\{(2n-1)\omega - 1\}N \right\} \quad (55)$$

### 3.2 Model-II : $f(Q) = \exp\{nQ\}$

In contrast to many higher order curvature based theories like  $f(R)$  etc.,  $f(Q)$  gravity leads to second order field equations which are similar to those produced by GR. Higher order time derivatives typically signal ghost instabilities, eg. Ostrogradsky ghosts. As exponential  $f(Q)$  model inherits this second order nature, it turns dynamically stable at the level of equations of motion. The first Friedmann equation becomes  $e^{6nH^2} (6nH^2 + \frac{1}{2}) = \rho$ . At late times,  $\rho \rightarrow 0$ , as matter dilutes. Now  $e^{6nH^2} > 0$  and  $6nH^2 + \frac{1}{2} \rightarrow 0$  which gives a real (positive) value of Hubble parameter as  $H^2 \rightarrow \frac{1}{12n}$ . This signifies that the Hubble parameter asymptotes to a constant, corresponding to deSitter expansion. This resembles cosmological constant. Also, the effective equation of state  $\omega_{eff} = -1 - \frac{2\dot{H}}{3H^2}$  turns  $-1$  at late time (as  $H \rightarrow \text{constant}$  and  $\dot{H} \rightarrow 0$ ). This also supports cosmological constant at late time. At small  $Q$ , i.e., small Hubble parameter, we can expand the function as,

$$f(Q) \approx 1 + nQ + \frac{(nQ)^2}{2!} + \dots \quad . \quad (56)$$

This reduces to GR when  $nQ \ll 1$ , making it easy to recover GR in an appropriate limits and controls the deviation. Depending on the sign and magnitude of  $n$ , the model can lead to bouncing cosmologies, deSitter solutions, phantom divergence free evolution, emergent universe scenarios and builds an outline to non-standard cosmological histories.

The exponential  $f(Q)$  model was tested against various cosmological datasets, including the Pantheon+ supernova compilation, Hubble parameter measurements and redshift space distortion data. The researchers employed a Markov Chain Monte Carlo (MCMC) analysis to numerically solve the modified Friedmann equations and constrain the model parameters. Their findings indicate that the exponential model provides a statistically better fit to the observational data compared to both the power law  $f(Q)$  model and the standard  $\Lambda$ CDM model, as evaluated using Bayesian and corrected Akaike Information Criteria[25].

For this model, we can express  $f_Q$  and  $f_{QQ}$  in terms of the dynamical variables as,

$$f_Q = ne^{nQ} \quad \text{and} \quad (57)$$

$$f_{QQ} = n^2 e^{nQ} \quad . \quad (58)$$

Substituting the value of  $f_Q$  in (34), we obtain,

$$Q = \frac{1}{n} \cdot \frac{1-z}{2(1-x-z)} \quad . \quad (59)$$

Now we can express the  $Q$ -derivatives of  $f(Q)$  in terms of the dynamical variables as,

$$f_Q = n \exp \left\{ \frac{1-z}{2(1-x-z)} \right\} \quad \text{and} \quad (60)$$

$$f_{QQ} = n^2 \exp \left\{ \frac{1-z}{2(1-x-z)} \right\} \quad . \quad (61)$$

Substituting the values of (60) and (61) in (28), we obtain,

$$\Gamma = \frac{f_Q}{Q f_{QQ}} = \frac{1}{nQ} = \frac{2(1-x-z)}{1-z} \quad . \quad (62)$$

Now by substituting the expression of  $\Gamma$  from (62), the dynamical equations reduced to,

$$x' = \frac{6x \{x^2(\omega+1) - 2x(\omega+1) + x(2\omega+3)z + (z-1)(-\omega+2z-1)\}}{x+2z-2} \quad \text{and} \quad (63)$$

$$z' = 6z(x\omega + x + z - 1) \quad . \quad (64)$$

For this particular model, the equation (32) is reduced to,

$$\frac{\dot{H}}{H^2} = - \frac{3 [x^2(\omega+1) + x \{-\omega + (2\omega+3)z - 1\} + 2(z-1)z]}{x+2z-2} \quad . \quad (65)$$

Different critical points and their categorizations are given in the table 2. In fig 2a to 2d,  $z$  vs  $x$  phase diagrams for different values of  $\omega$  are drawn.

Stable hyperbolic nodes are followed which corresponds to a deSitter like state where scale factor grows exponentially ( $\approx e^{H(z)}$ ). This aligns with attempts to explain cosmic acceleration via pure gravity modifications. Matter energy density  $\Omega \rightarrow 0$  at stable nodes [26]. Anisotropy variables decay and the universe isotropizes and becomes matter diluted at late times. Formation of such node improves the predictive stability of the theory across cosmological scales.

Hyperbolic saddle generally denotes matter or radiation dominated phases.  $\Omega_m$  is dominant in this case and the shear may decay slowly. These epochs are required for structure formation and CMB consistency. Saddles ensure that the universe passes through standard observable stages like matter domination, before exiting towards a DE dominated future. In  $f(Q) = \exp\{nQ\}$ , the exponential term gradually becomes dominant at low curvature ( $Q \rightarrow 0$ ). Saddle behavior allows the system to stay long enough in matter dominated phase and then naturally exit towards a stable attractor, typically which is a deSitter node. This

Crit. Point	Existence	Eigenvalues	Type of crit. point	Stability	Cosmology
$x \rightarrow 0$	$\forall \omega$	$-3(\omega + 1)$ and $-6$	Hyperbolic ( $\omega \neq -1$ )	Stable node for $\omega > -1$	$a(t) = a_0 e^{H_0 t}$ (i.e., deSitter)
				Saddle Point for $\omega < -1$	
			Non-hyperbolic ( $\omega = -1$ )	Center Manifold for $\omega = -1$	
$x \rightarrow 1$	$\forall \omega$	0 and $6\omega$	Non-hyperbolic ( $\forall \omega$ )	Fully degenerate for $\omega = 0$	$a(t) = a_0 e^{H_0 t}$ (i.e., deSitter)
				Center Manifold for $\omega > 0$ and $\omega < 0$	

Table 2: Critical points with existence conditions, eigen values, type of critical points, stability and cosmology pattern for model-II:  $f(Q) = \exp\{nQ\}$

provides a graceful exit mechanism to late time acceleration without fine tuning. In an anisotropic Bianchi-I model, a saddle point may include non-zero shear[27]. The eigenvalues control whether anisotropy decays (via negative eigenvalues) to isotropization or grows to instability. If shear decays, the saddle supports early anisotropic evolution that transits to isotropy – consistent with observational constraints.

Saddle points connect unstable early time nodes( like Big Bang) to stable late time deSitter like attractors. These fixed points act as a cosmic way point that funnels trajectories toward the realistic evolution path.

In table 2, we also observe that the possibility of formation of a center manifold, when  $\omega = -1$ . In cosmology, generally, this corresponds to slow, delicate evolution where the universe may linger near such a regime and small changes in parameters can lead to dramatically different outcomes. The center manifold typically hosts trajectories that slowly evolve, remaining close to a fixed point for extended periods. Cosmologically, a quasi-deSitter state resembles ultra-slow roll inflation or early time acceleration [28]. A center manifold indicates that the system is at the edge of bifurcation. Small changes in initial conditions or parameters could lead to a stable deSitter future or collapse or oscillatory/cyclic behavior or to exit towards anisotropic Bianchi-I type attractors. In Bianchi-I models, the center manifold can host solutions where shear slowly decays or remains nearly constant. It models a universe that becomes more homogeneous gradually due to geometry.

When  $x \rightarrow 1$  and  $\omega = 0$ , we find the existence of a fully degenerate fixed point. The Jacobian matrix turns nilpotent at this point. It is non-hyperbolic and linear stability analysis breaks down. Typically, this signals the onset of a bifurcation, a phase transition or a critical behavior. Cosmologically, a sensitive region is signified where small changes in parameters generate bifurcation points where new attractor solutions appear or existing ones disappear. These attractors can be deSitter, power law inflation, cyclic or other exotic geometries. A geometric realisation of non-singular cosmological models without requiring extra matter content is followed from such fixed points. Even this may model an ultra slow roll inflationary epoch or a prolonged quasi deSitter phase, naturally arising from the gravitational dynamics.

Time-time perturbation for this model emerges as

$$6ne^{nQ}(\dot{\Psi} + H\Phi) + n^2 e^{nQ} \delta Q = \delta \rho \quad , \quad (66)$$

where  $\delta Q = 12H(\dot{\Psi} + H\Phi)$ .

Space-space perturbation, on the other hand produces

$$2ne^{nQ}(\dot{\Psi} + H\Phi) + n^2 e^{nQ}(\dot{Q}\Psi + Q\dot{\Psi}) = -a^2 \delta p \quad , \quad (67)$$

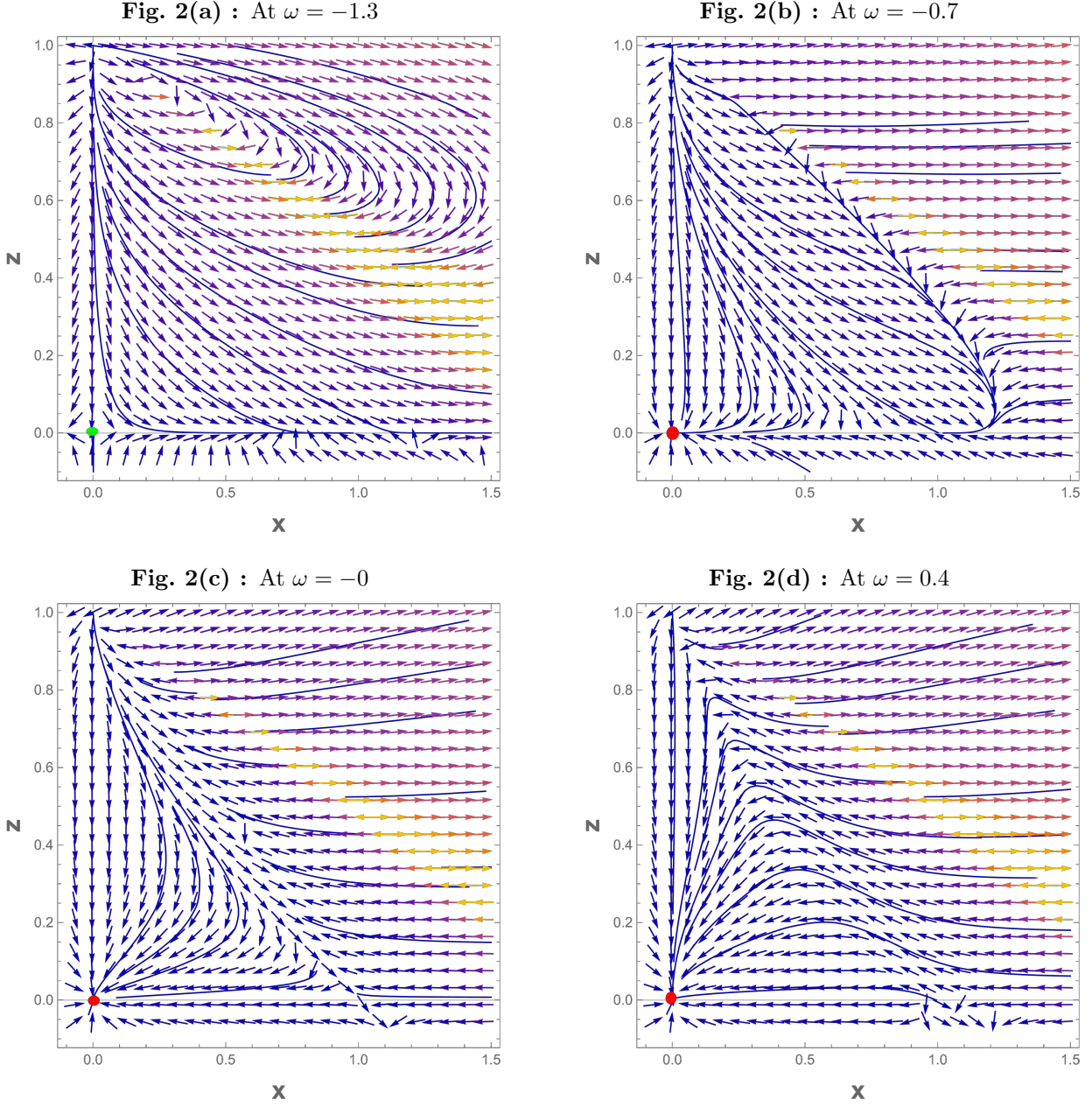


Figure 2: Figure (a) – (d) are  $z$  vs  $x$  phase diagrams for the model  $f(Q) = \exp\{nQ\}$  at different values of  $\omega$ . A red dot indicates a stable point, a green dot indicates a saddle point and a blue dot indicates an unstable point.

where the non-metricity perturbation  $\delta Q$  is,

$$\delta Q = 12H(\dot{\Psi} + H\Phi) . \quad (68)$$

The propagation speed of scalar perturbation is,

$$C_s^2 = \frac{1 + n\frac{\dot{Q}}{H}}{1 + 2nQ} . \quad (69)$$

The stability occurs when  $C_s^2 > 0$ , if  $n > 0$  and the no ghost condition holds if  $n > 0$ . The tensor modes propagate with the speed is,

$$C_T^2 = \frac{1}{1 + 2nQ} \quad . \quad (70)$$

For  $C_T^2 \approx 1$  (as in GR), we require  $2nQ \ll 1$ .

### 3.3 Model-III : $f(Q) = \alpha Q^2 + vQ^2 \log(Q)$

This model is inspired by quantum corrections, especially the logarithmic term arises in loop expansions [29, 30] Effective field theories, where logarithmic corrections are expected at high curvature regimes are also driving motivations. In Bianchi-I metric, shear or anisotropy enters via

$$\sigma^2 = \frac{1}{2} \sum_{i=1}^3 (H_i - H)^2 \quad \text{and}$$

the non-metricity scalar  $Q$  is generalised to  $Q = 6H^2 + \text{shear}$  corrections. At high  $Q$ , the  $Q^2 \log Q$  term becomes dominant to drive inflation like dynamics. Effective equilibrium of state  $\omega_{eff} \rightarrow -1$  (quasi deSitter) and anisotropy  $\sigma^2$  decays over time. When matter dominated decelerated expansion is going on or when the anisotropy slowly decays (matching CMB constraints), we expect saddle. As  $Q \rightarrow 0+$ ,  $Q^2 \log Q \rightarrow 0$  and hence depending on the value of  $\alpha$ , stable deSitter attractor or phantom like regime ( $\omega_{eff} < -1$ ) may be followed.

Now, for this model, we can calculate the  $Q$ -derivatives as,

$$f_Q = (2\alpha + v)Q + 2Qv \log(Q) \quad \text{and} \quad (71)$$

$$f_{QQ} = (2\alpha + 3v) + 2v \log(Q) \quad . \quad (72)$$

Substituting the values of  $f_Q$  and  $f_{QQ}$  in equation (34), we get,

$$\log(Q) = \frac{\alpha(-4x - 3z + 3) + 2v(x + z - 1)}{v(4x + 3z - 3)} \quad . \quad (73)$$

Similarly, we can calculate the expression of  $\Gamma$ , given by,

$$\Gamma = \frac{8x + 7z - 7}{16x + 13(z - 1)} \quad . \quad (74)$$

Now, by substituting the values of  $\Gamma$ , the dynamical variables are reduced to,

$$x' = 3x \left[ \frac{2x(\omega + 1) \{16x + 13(z - 1)\}}{(z - 1) \{40x + 33(z - 1)\}} + 2(x\omega + x + z) - \omega - 1 \right] \quad \text{and} \quad (75)$$

$$z' = 6z(x\omega + x + z - 1) \quad . \quad (76)$$

Also for this model, the equation (29) reduces to,

$$\frac{\dot{H}}{H^2} = - \frac{3 [8x^2(\omega + 1)(5z - 1) + x(z - 1) \{ (33\omega + 73)z - 7(\omega + 1) \} + 33(z - 1)^2 z]}{(z - 1) \{40x + 33(z - 1)\}} \quad . \quad (77)$$

We enlist all the fixed points and their categorizations in table 3. Figure 3(a)-3(d) are plots of  $x - z$  plane phase portraits for different  $\omega$  values. At the same time, two stable nodes and two unstable nodes are observed to form. For one stable point, the dynamical system admits a fixed point where the Hubble parameter  $H$  becomes constant or anisotropy turns to vanish or matter density decays. Two distinct stable

Crit. Point	Existence	Eigenvalues	Type of crit. point	Stability	Cosmology
$x \rightarrow 0, z \rightarrow 0$	$\forall \omega$	$-6$ and $-3(\omega + 1)$	Hyperbolic ( $\omega \neq -1$ )	Stable node for $\omega > -1$	$a(t) = a_0 e^{H_0 t}$ (i.e., deSitter)
				Saddle Point for $\omega < -1$	
			Non-hyperbolic ( $\omega = -1$ )	Center Manifold for $\omega = -1$	
$x \rightarrow \frac{3}{4}, z \rightarrow 0$	$\forall \omega$	$6(\omega + 1)$ and $\frac{3}{2}(3\omega - 1)$	Hyperbolic ( $\omega \neq -1, \frac{1}{3}$ )	Stable node for $\omega < -1$	$a \propto t^{\frac{4}{3(1+\omega)}}$
				Saddle point for $-1 < \omega < \frac{1}{3}$	
				Unstable node for $\omega > \frac{1}{3}$	
			Non-hyperbolic ( $\omega = -1, \frac{1}{3}$ )	Center manifold for $\omega = -1, \frac{1}{3}$	
$x \rightarrow \frac{11}{12}, z \rightarrow 0$	$\forall \omega$	$6(\omega + 1)$ and $\frac{1}{2}(11\omega - 1)$	Hyperbolic ( $\omega \neq -1, \frac{1}{11}$ )	Stable node for $\omega < -1$	$a \propto t^{\frac{4}{1+\omega}}$
				Saddle point for $-1 < \omega < \frac{1}{11}$	
				Unstable node for $\omega > \frac{1}{11}$	
			Non-hyperbolic ( $\omega = -1, \frac{1}{11}$ )	Center manifold for $(\omega = -1, \frac{1}{11})$	

Table 3: Critical points with existence conditions, eigenvalues, type of critical points, stability and cosmology pattern for model-III:  $f(Q) = \alpha Q^2 + vQ^2 \log(Q)$

points can exist when multiple zeros of the effective equation governing  $\dot{H}$  are there. Multiple physically allowed solutions for  $H$  or  $Q$ , i.e., multiple deSitter like attractor may appear. The term  $Q^2 \log Q$  introduces turning point and the equation  $2f_Q + Qf_{QQ} = 0$  may have two real positive roots for  $Q$ . On the other hand, the model may include a non-trivial matter sector or anisotropic shear and then one attractor could correspond to matter scaling solution, i.e., deceleration with small anisotropy. Another stable point could be a pure deSitter attractor with isotropic expansion[31, 32]. Two unstable points may rise due to multiple early time solutions. One of them may correspond to a high  $Q$  regime (large Hubble rate), i.e., early inflation. Another may lie at moderate  $Q$ , representing a matter like or stiff fluid like phase. In presence of double unstable points, the universe is followed to evolve following multiple paths (bifurcation structure) which is similar as the authors of [28] have followed.

Time-time perturbation for this model is given by,

$$6H\{(2\alpha + v)Q + 2vQ \log Q\}(\dot{\Psi} + H\Phi) + \{(2\alpha + v) + 2v \log Q + 2v\}\delta Q = \delta\rho \quad \text{and} \quad (78)$$

space-space perturbation is given by,

$$2\{(2\alpha + v)Q + 2vQ \log Q\}(\dot{\Psi} + H\Phi) + \{(2\alpha + v) + 2v \log Q + 2v\}(\dot{Q}\Psi + Q\dot{\Psi}) = -a^2\delta p \quad , \quad (79)$$

where  $\delta Q$  is the non-metricity perturbation given by,

$$\delta Q = 12H(\dot{\Psi} + H\Phi) \quad (80)$$

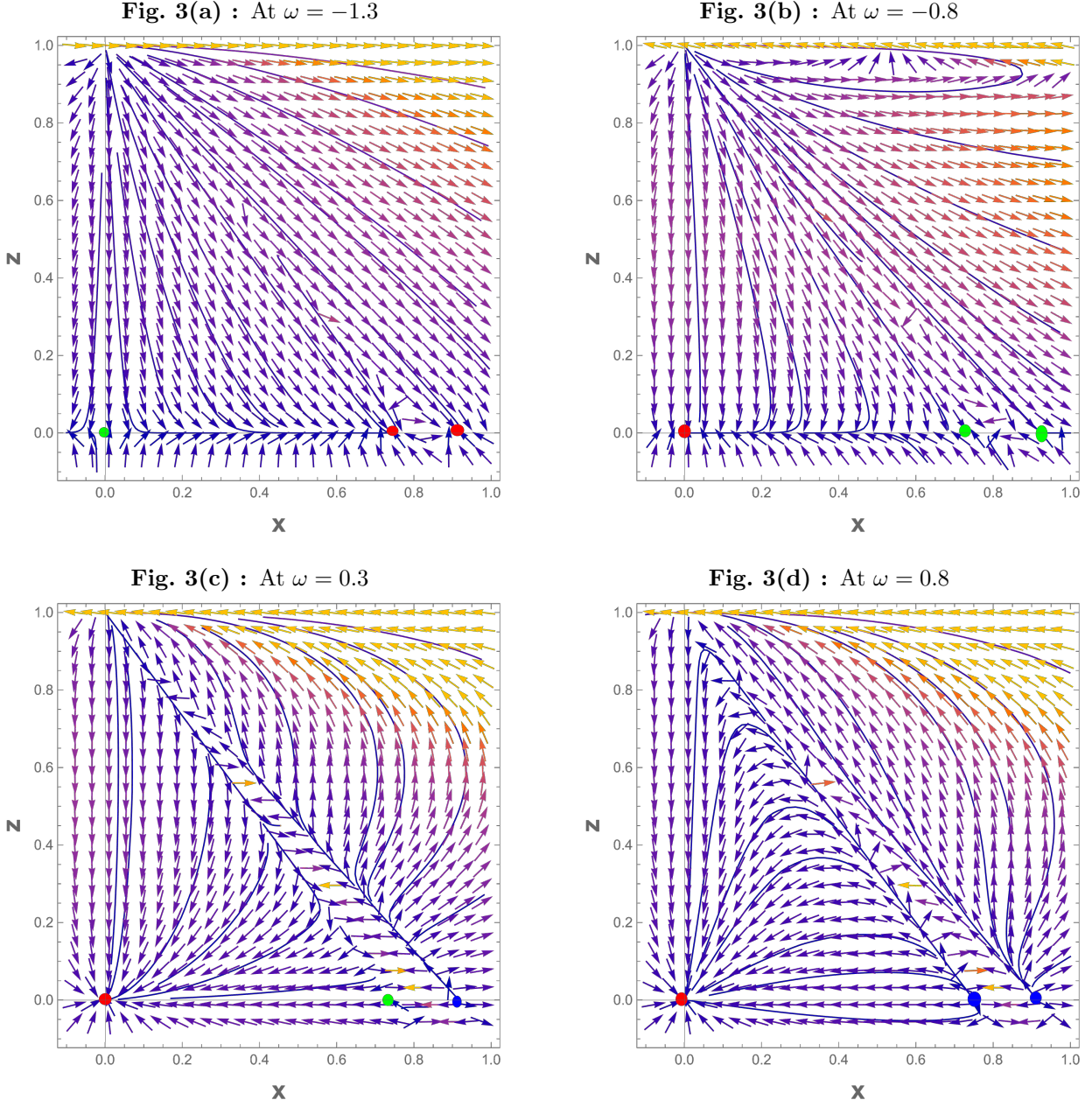


Figure 3: Figure (a) – (d) are  $z$  vs  $x$  phase diagrams for the model  $f(Q) = \alpha Q^2 + vQ^2 \log(Q)$  at different values of  $\omega$ . A red dot indicates a stable point, a green dot indicates a saddle point and a blue dot indicates an unstable point.

The propagation speed of scalar perturbation is,

$$C_s^2 = \frac{2HQ(v + 2\alpha) + \dot{Q}(3v + 2\alpha) + 2(2HQ + \dot{Q})v \log Q}{6H^3\{(6 + Q)v + 2(2 + Q)\alpha + 2(2 + Q)v \log Q\}} \quad , \quad (81)$$

stability occurs when  $C_s^2 > 0$  and subliminal when  $C_s^2 \leq 1$ .

No ghost condition is given by,

$$(2\alpha + v)Q + 2vQ \log Q > 0 \quad . \quad (82)$$

The speed of gravitational waves is

$$C_T^2 = \frac{v + 2\alpha + 2v \log Q}{7v + 6\alpha + 6v \log Q} . \quad (83)$$

For consistency with (i.e;  $C_T^2 = 1$ ), we require,

$$2Qf_{QQ} \ll f_Q . \quad (84)$$

### 3.4 Model-IV : $f(Q) = \eta Q_0 \sqrt{\frac{Q}{Q_0}} \log \left( \frac{\lambda Q_0}{Q} \right)$

The fractional power  $Q^{\frac{1}{2}}$  dominates at low curvature at late times. A logarithmic correction  $\log \left( \frac{Q_0}{Q} \right)$  is reminiscent of quantum loop or renormalisation corrections [33]. A prefactor  $\eta Q_0$  sets a cosmological scale. Such structure arises in nonlocal or scale dependent gravity, renormalisation group which improves effective actions. This models with conformal anomalies or vacuum polarisation. In Bianchi-I, where shear evolves as  $\dot{\sigma} + 3H\sigma$ , the slowly decaying logarithmic correction modifies the friction term for shear[34].

Here,  $\eta$  is a dimensionless constant,  $Q_0$  is a constant scale of non-metricity,  $\lambda$  is a dimensionless parameter and  $Q$  is the non-metricity scalar. The  $Q$ -derivatives of the model are,

$$f_Q = \frac{\eta}{2} \sqrt{\frac{Q_0}{Q}} \left\{ \log \left( \frac{\lambda Q_0}{Q} \right) - 2 \right\} \quad \text{and} \quad (85)$$

$$f_{QQ} = -\frac{1}{4} \frac{\eta}{Q} \sqrt{\frac{Q_0}{Q}} \log \left( \frac{\lambda Q_0}{Q} \right) . \quad (86)$$

Substituting the value of  $f_Q$  in equation (34), we obtain,

$$\log \left( \frac{\lambda Q_0}{Q} \right) = \frac{2(1-z)}{4x+3z-3} . \quad (87)$$

Substituting the values of equations (85) and (86) we can easily find the value of  $\Gamma$  as,

$$\Gamma = \frac{8(x+z-1)}{1-z} . \quad (88)$$

Now the dynamical variables are reduced to,

$$x' = 3x \left( \frac{x(\omega+1)}{-4x-3z+3} + 2(x\omega+x+z) - \omega - 1 \right) , \quad (89)$$

$$z' = 6z(x\omega+x+z-1) \quad \text{and} \quad (90)$$

equation (32) reduced to,

$$\frac{\dot{H}}{H^2} = -\frac{3(4x^2(\omega+1) - 4x(\omega+1) + x(3\omega+7)z + 3(z-1)z)}{4x+3z-3} . \quad (91)$$

In table 4, different critical points and their categorizations are noted. Fig 4a – 4d are  $z$  vs  $x$  phase diagrams for different values of  $\omega$ . At the same time, stable, unstable and saddle nodes are found to form. Multiple deSitter like attractors i.e., physically acceptable solutions appear. deSitter solutions appear at  $x \rightarrow 0$  and  $x \rightarrow -1$  for different critical point, suggesting that model IV supports the accelerating expansion as stable or unstable phases. Late time cosmic acceleration as a deSitter attractor is found at  $x \rightarrow 0$  and the possible inflationary era as a deSitter solution is formed at  $x \rightarrow 1$ . A  $x \rightarrow \frac{3}{8}$  power-law expansion appears, which may correspond to matter/radiation dominated era depending on the values of  $\omega$ . The stability

Crit. Point	Existence	Eigenvalues	Type of crit. point	Stability	Cosmology
$x \rightarrow 0, z \rightarrow 0$	$\forall \omega$	$-3(\omega + 1)$ and $-6$	Hyperbolic ( $\omega \neq -1$ )	Saddle for $\omega < -1$	$a(t) = a_0 e^{H_0 t}$ (i.e., deSitter)
				Stable Node for $\omega > -1$	
			Non-hyperbolic ( $n = -1$ )	Center manifold for $\omega = -1$	
$x \rightarrow \frac{3}{8}, z \rightarrow 0$	$\forall \omega$	$\frac{3}{4}(3\omega - 5)$ and $\frac{15}{4}(\omega + 1)$	Hyperbolic ( $\omega \neq -1, \frac{5}{3}$ )	Stable Node for $\omega < -1$	$a \propto t^{\frac{8}{15(1+\omega)}}$
				Saddle point for $-1 < \omega < \frac{5}{3}$	
				Unstable Node for $\omega > \frac{5}{3}$	
			Non-hyperbolic ( $\omega = -1, \frac{5}{3}$ )	Center manifold for $\omega \neq -1, \frac{5}{3}$	
$x \rightarrow 1, z \rightarrow 0$	$\forall \omega$	$6\omega$ and $15(\omega + 1)$	Hyperbolic ( $\omega \neq -1, 0$ )	Stable node for $\omega < -1$	$a(t) = a_0 e^{H_0 t}$ (i.e., deSitter)
				Saddle point for $-1 < \omega < 0$	
				Unstable node for $\omega > 0$	
			Non-hyperbolic ( $\omega = -1, 0$ )	Center manifold for $\omega = -1, 0$	

Table 4: Critical points with existence conditions, eigenvalues, type of critical points, stability and cosmology pattern for model-IV :  $f(Q) = \eta Q_0 \sqrt{\frac{Q}{Q_0}} \log\left(\frac{\lambda Q_0}{Q}\right)$

of each phase depends strongly on the EoS  $\omega$ , i.e., this model can describe different cosmological epochs dynamically. The non-hyperbolic points correspond to the bifurcation or marginal stability. So these points required the center manifold or higher order analysis.

Like model III, model IV is also observed to possess two stable or two unstable fixed nodes at a time. They are followed to lie on  $z = 0$  axis.

The time-time perturbation emerges as,

$$3Hn\sqrt{\frac{Q_0}{Q}} \left\{ \log \frac{\lambda Q_0}{Q} - 2 \right\} \{(\dot{\Psi} + H\Phi)\} - \frac{n\sqrt{Q_0} \log\left(\frac{\lambda Q_0}{Q}\right)}{4Q^2} \delta Q = \delta \rho \quad . \quad (92)$$

Space-space perturbation is given by,

$$n\sqrt{\frac{Q_0}{Q}} \left\{ \log \left( \frac{\lambda Q_0}{Q} \right) - 2 \right\} (\dot{\Psi} + H\Phi) - \frac{n\sqrt{Q_0}}{4Q^{\frac{3}{2}}} \log \left( \frac{\lambda Q_0}{Q} \right) \times (\dot{Q}\Psi + Q\dot{\Psi}) = -a^2 \delta p \quad , \quad (93)$$

where  $\delta Q$  is the non-metricity perturbation given by  $\delta Q = 12H(\dot{\Psi} + H\Phi)$ . The propagation speed of scalar perturbation is,

$$C_s^2 = \frac{8HQ + (\dot{Q} - 4HQ) \log\left(\frac{\lambda Q_0}{Q}\right)}{12H^2 \left\{ 2Q + (H - Q) \log\left(\frac{\lambda Q_0}{Q}\right) \right\}} \quad . \quad (94)$$

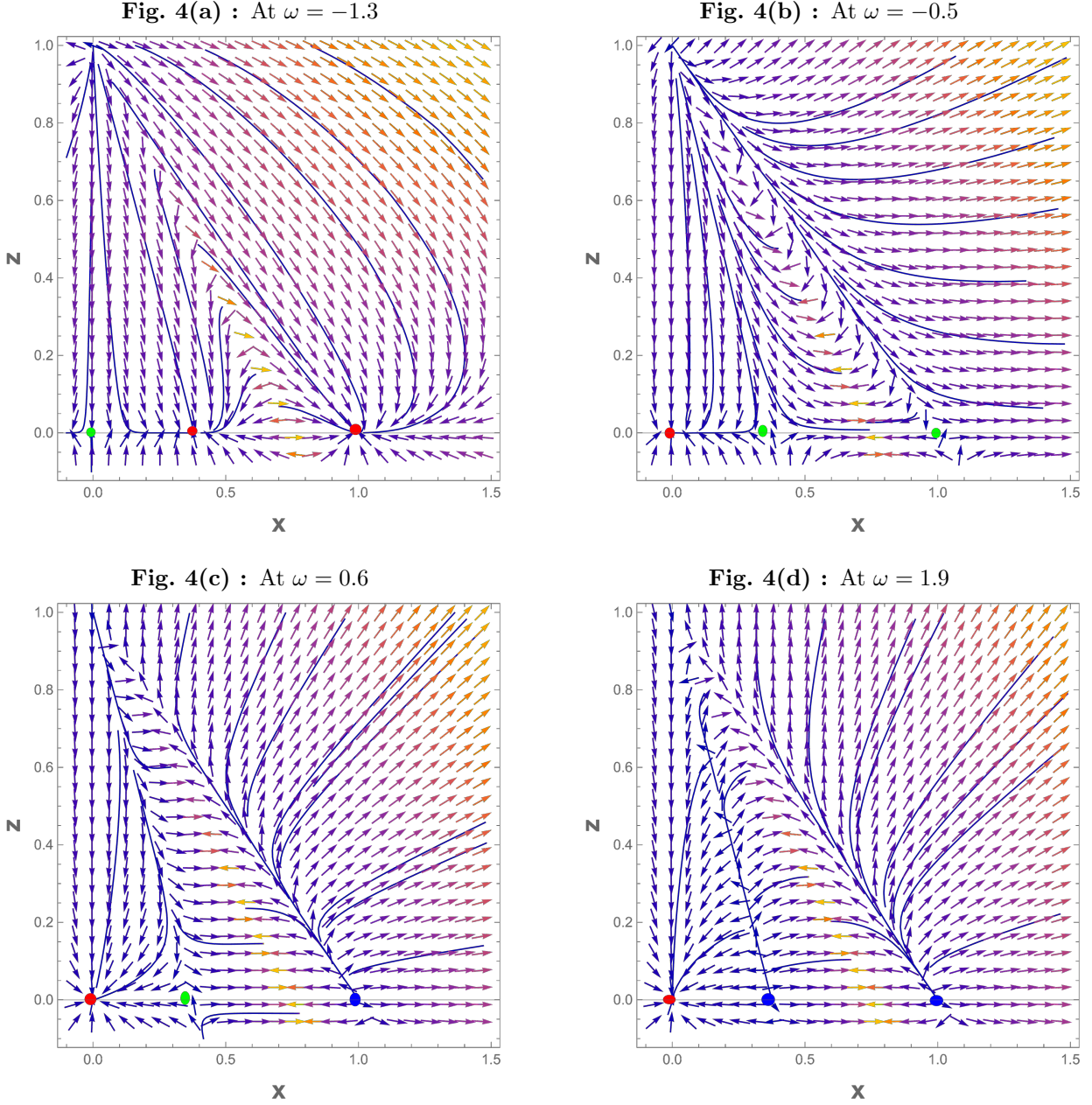


Figure 4: Figure (a) – (d) are  $z$  vs  $x$  phase diagrams for the model  $f(Q) = \eta Q_0 \sqrt{\frac{Q}{Q_0}} \log\left(\frac{\lambda Q_0}{Q}\right)$  at different values of  $\omega$ . A red dot indicates a stable point, a green dot indicates a saddle point and a blue dot indicates an unstable point.

For stability condition  $0 \leq C_s^2 \leq 1$ , no ghost condition is  $\frac{n}{2} \sqrt{\frac{Q_0}{Q}} \left\{ \log\left(\frac{\lambda Q_0}{Q}\right) - 2 \right\} > 0$  and the speed of gravitational waves is,

$$C_T^2 = \frac{\log\left(\frac{\lambda Q_0}{Q}\right) - 2}{4} . \quad (95)$$

For  $C_T^2 \approx 1$  (as in GR), we required,  $\log\left(\frac{\lambda Q_0}{Q}\right) \approx 2 \Rightarrow Q \approx \lambda Q_0 e^2$ , which may conflict with the no-ghost condition unless  $\lambda$  is fine-tuned.

## 4 Brief Discussion and Conclusion

Early universe measurements of the value of Hubble parameter differs from the same measured for late time universe. Hubble tension measured thus suggests regarding the incompleteness of standard general relativity or cosmological principle. Different voids, temperature fluctuations, dipole modulation, anisotropic inflation etc points towards anisotropic universe. A curvature-free torsion-free gravity is chosen. The signature entity will be the non-metricity scalar  $Q$ . It is followed that this gravity theory, depending on different free parameters of the model, can fit early inflation to late time cosmic acceleration. No need to modify the stress energy tensor part of field equation with any exotic fluid is required. Our motive was to analysis different fixed points of the phase portraits constructed upon this model. For this, some model parameters are carefully chosen so that their derivatives are found to linearly depend on the same set of parameters. Vanishing derivatives indicates extremality and hence we check for singular properties of the corresponding Jacobian matrix is followed to point properties and classifications of the fixed/ critical points. Cosmological implications are investigated.

First gravity model chosen with non-metricity scalar is  $f(Q) = mQ^n$ . This mimics general relativity for  $m = n = 1$ .  $n > 1$  is able to reproduce early inflation. For  $0 < n < 1$ , however, gravity gets weakened and can be interpreted as the effect of a repulsive force, i.e., the late time cosmic acceleration is made after. This model can predict gravitational waves to propagate with the speed of light which is supported by GW170817 event [22]. We have enlisted the fixed points for this model in table 1 and phase portraits are emphasised in fig 1a-1d. We find hyperbolic stable, unstable nodes and saddles. Non-hyperbolic critical point, for this model comes as a center manifold. Among these, the hyperbolic stable point, formed near the origin in all phase portraits signifies that the universe should always end up in the same state. This also explains why today's universe is isotropic to a large scale and accelerating. Also stable point corresponding to  $x = 0$  indicates constant Hubble parameter and hence a late time acceleration.

In Bianchi-I, a saddle point having non-zero anisotropy can start from an anisotropic state and exit towards an isotropic attractor. Hyperbolic unstable points may indicate that the universe starts near this kind of points (eg, anisotropic inflation), strong repulsion may cause nearby trajectories to diverge rapidly and create an unstable fixed point. Shear variable from anisotropic contribution can lead so. Lastly, we must remember, an unstable node not only be thought to express late time attractor. It may also signify a past attractor as well.

In the second model,  $f(Q) = e^{nQ}$  in Bianchi-I cosmology provides a minimal, purely geometric mechanism for explaining the universe's anisotropic origin and accelerated fate, all within a unified, covariant and second order field theory.  $f(Q) = e^{nQ}$  grows rapidly, so does  $f_Q$ , leading to strong geometric feedback on the shear evolution. If matter is subdominant and  $n > 0$ , shear decays but slowly which implies anisotropic inflation. Linear perturbations grow away from this node such that the system exists anisotropic phase naturally. Besides such unstable points, if we look towards stable nodes, we follow the shear equation  $\dot{\sigma} + 3h\sigma \approx 0$  and to imply  $\sigma \propto e^{-3ht}$  and the universe ends in a fully isotropic accelerated expansion, consistent with CMB constraints. At late time shear vanishes to restore isotropy.

In this model, fully degenerate fixed point is found. Hartman Grobman theorem does not apply for these points. Trajectories near this point behave non-linearly. Universe near such points may exhibit slow evolution, neither accelerating nor decelerating strongly. Small anisotropy and matter or quantum fluctuations may push towards different attractors. This may again represent bifurcation thresholds, eg., transition from isotropic to anisotropic solutions or inflation to matter era.

A center manifold is also observed to form. This lies in the shear direction while other parameters are stable. Here shear neither grows nor decays first. Universe remains mildly anisotropic. Higher order corrections regulate whether the universe becomes isotropic later or not. Universe could hover near the manifold, mimicking near-isotropic expansion.

The third model considered is  $f(Q) = \alpha Q^2 + vQ^2 \log Q$ . If  $Q$  is small and positively vanishes,  $Q^2 \log Q$  term also does so and  $Q^2$  dominates representing a deSitter attractor/phantom. At high  $Q$ , inflation like dynamics is expected. While finding and categorizing fixed points, both hyperbolic and non-hyperbolic fixed

points are seen to be formed. More than one stable points are followed. One of them is a stable node which signifies early inflation like quasi deSitter phase. Another is a stable spiral pointing towards late time DE dominated deSitter space. Geometric tracking solutions are interpreted by centers. In a phase portrait, we have followed two unstable nodes. One may signify the early universe saddle for high shear and the rest one may be caused by inflationary node. The actual trajectory should depend on the initial shear, matter content and the sign of different model parameters.

Last studied model is  $f(Q) = \eta Q_0 \sqrt{\frac{Q}{Q_0}} \log\left(\frac{\lambda Q_0}{Q}\right)$ . In the Bianchi-I universe, chosen model provides a compelling geometric framework for exploring anisotropic cosmology, combining the effects of square-root and logarithmic non-metricity terms. Physically, it allows the universe to transit smoothly from an early anisotropic matter dominated phase to a late-time accelerated and isotropic expansion without invoking dark energy fields. The logarithmic correction enhances the model's flexibility at low  $Q$  (late times), enabling deSitter like behavior, while the square root term ensures controlled dynamics at high  $Q$  (early times). In the Bianchi-I background, it governs the decay of anisotropy, potentially hosting stable attractors and metastable center manifolds that regulate cosmic evolution. Such a model is valuable for explaining cosmic acceleration, isotropization and transitions between epochs entirely through gravitational geometry, making it a strong candidate for a unified description of the universe's expansion history. Overall, the dynamical model matches the same for the third model to a large extent.

## Acknowledgements

RB and FR thank IUCAA, Pune for the Visiting Associateship. Also, FR thanks ANRF, SERB, Government of India, for financial support.

## Data Availability Statement

My manuscript has no associated data. [Authors' comment: The authors have not used any data in the manuscript. The authors have only compared the results with already openly available cosmological results.]

## Conflict of Interest

There are no conflicts of interest.

## Funding Statement

There is no funding to report for this article.

## References

- [1] Planck Collaboration, “Planck 2018 results. vi. cosmological parameters,” *Astronomy & Astrophysics*, vol. 641, p. A6, 2020.
- [2] A. G. Riess, S. Casertano, W. Yuan, L. M. Macri, and D. Scolnic, “A comprehensive measurement of the local value of the hubble constant with  $1 \text{ km s}^{-1} \text{ mpc}^{-1}$  uncertainty from the hubble space telescope and the sh0es team,” *The Astrophysical Journal*, vol. 934, no. 1, p. L7, 2022.
- [3] P. Collaboration, N. Aghanim, Y. Akrami, *et al.*, “Planck 2018 results. i. overview and the cosmological legacy of planck,” *Astronomy & Astrophysics*, vol. 641, p. A1, 2020.
- [4] N. Aghanim *et al.*, “Planck 2018 results. vi. cosmological parameters,” *Astron. Astrophys*, vol. 641, p. A6, 2020.
- [5] H. K. Eriksen, F. K. Hansen, A. J. Banday, K. M. Górski, and P. B. Lilje, “Asymmetries in the cosmic microwave background anisotropy field,” *The Astrophysical Journal*, vol. 605, no. 1, p. 14, 2004.
- [6] A. Kovács, I. Szapudi, B. R. Granett, Z. Frei, J. Silk, W. Burgett, S. Cole, P. W. Draper, D. J. Farrow, N. Kaiser, *et al.*, “Supervoid origin of the cold spot in the cosmic microwave background,” *Proceedings of the International Astronomical Union*, vol. 10, no. S306, pp. 269–272, 2014.
- [7] S. Rathore and S. S. Singh, “Stability aspects of an lrs bianchi type-i cosmological model in  $f(q)$  gravity,” *General Relativity and Gravitation*, vol. 56, no. 25, 2024.
- [8] A. Paliathanasis and G. Leon, “Bianchi i spacetimes in  $f(q)$ -gravity,” *arXiv preprint arXiv:2406.04563*, 2024. 24 pages, no figures.
- [9] M. Hohmann, “General covariant symmetric teleparallel cosmology,” *Physical Review D*, vol. 104, no. 12, p. 124077, 2021.
- [10] C. G. Böhm, E. Jensko, and R. Lazkoz, “Cosmological dynamical systems in modified gravity,” *The European Physical Journal C*, vol. 82, no. 6, p. 500, 2022.
- [11] H. Shabani, A. De, and T.-H. Loo, “Phase-space analysis of a novel cosmological model in  $f(q)$  theory,” *The European Physical Journal C*, vol. 83, no. 6, p. 535, 2023.
- [12] A. Paliathanasis, “Dynamical analysis of  $f(q)$ -cosmology,” *Physics of the Dark Universe*, vol. 41, p. 101255, 2023.
- [13] H. Shabani, A. De, T.-H. Loo, and E. N. Saridakis, “Cosmology of  $f(q)$  gravity in non-flat universe,” *The European Physical Journal C*, vol. 84, no. 3, p. 285, 2024.
- [14] F. Esposito, S. Carloni, and S. Vignolo, “Bianchi type-i cosmological dynamics in  $f(Q)$  gravity: a covariant approach,” *arXiv preprint arXiv:2207.14576*, 2022.
- [15] P. Sarmah and U. D. Goswami, “Dynamical system analysis of lrs-bi universe with  $f(q)$  gravity theory,” *Physics of the Dark Universe*, vol. 46, p. 101556, 2024.
- [16] T. Harko, T. S. Koivisto, F. S. Lobo, G. J. Olmo, and D. Rubiera-Garcia, “Coupling matter in modified  $q$  gravity,” *Physical Review D*, vol. 98, no. 8, p. 084043, 2018.
- [17] N. Frusciante, “Signatures of  $f(Q)$ -gravity in cosmology,” *Physical Review D*, vol. 103, no. 4, p. 044021, 2021.
- [18] S. Capozziello and K. F. Dialektopoulos, “Anisotropic cosmologies in modified gravity,” *European Physical Journal C*, vol. 81, p. 754, 2021.

- [19] S. Mandal, “Accelerated expansion of the universe in non-minimally coupled gravity,” *arXiv preprint arXiv:2301.02565*, 2023.
- [20] W. Khyllep and J. Dutta, “Cosmological solutions and growth index of matter perturbations in  $f(q)$  gravity,” *Physical Review D*, vol. 103, no. 10, p. 103521, 2021.
- [21] R. Lazkoz, F. S. Lobo, M. Ortiz-Baños, and V. Salzano, “Observational constraints of  $f(q)$  gravity,” *Physical Review D*, vol. 100, no. 10, p. 104027, 2019.
- [22] J. Beltrán Jiménez, L. Heisenberg, and T. Koivisto, “Coincident general relativity,” *Phys. Rev. D*, vol. 98, no. 4, p. 044048, 2018.
- [23] S. Mandal, D. Wang, and P. K. Sahoo, “Cosmography in  $f(q)$  gravity,” *Physical Review D*, vol. 102, no. 12, p. 124029, 2020.
- [24] S. Bahamonde, K. F. Dialektopoulos, C. Escamilla-Rivera, G. Farrugia, V. Gakis, M. Hendry, M. Hohmann, J. L. Said, J. Mifsud, and E. D. Valentino, “Teleparallel gravity: from theory to cosmology,” *Reports on Progress in Physics*, vol. 86, no. 2, p. 026901, 2023.
- [25] D. Mhamdi, F. Bargach, S. Dahmani, A. Bouali, and T. Ouali, “Constraints on power law and exponential models in  $f(q)$  gravity,” *Physics Letters B*, vol. 859, p. 139113, 2024.
- [26] N. Frusciante, “Modified gravity theories and cosmology: An introduction,” *Reports on Progress in Physics*, vol. 85, no. 8, p. 086901, 2022.
- [27] D. A. B. Iozzo, N. Khera, L. C. Stein, K. Mitman, M. Boyle, N. Deppe, F. Hébert, L. E. Kidder, J. Moxon, H. P. Pfeiffer, M. A. Scheel, S. A. Teukolsky, and W. Throwe, “Comparing remnant properties from horizon data and asymptotic data in numerical relativity,” *Physical Review D*, vol. 103, no. 12, p. 124029, 2021.
- [28] P. Prasia and V. C. Kuriakose, “Quasinormal modes and thermodynamics of nonsingular black holes in conformal gravity,” *General Relativity and Gravitation*, vol. 48, no. 7, p. 89, 2016.
- [29] N. D. Birrell and P. C. W. Davies, *Quantum Fields in Curved Space*. Cambridge Monographs on Mathematical Physics, Cambridge University Press, 1982.
- [30] S. Nojiri and S. D. Odintsov, “Modified gravity with  $\ln r$  terms and cosmic acceleration,” *General Relativity and Gravitation*, vol. 36, no. 8, pp. 1765–1780, 2004.
- [31] S. Bahamonde, K. F. Dialektopoulos, C. Escamilla-Rivera, G. Farrugia, V. Gakis, M. Hendry, M. Hohmann, J. L. Said, J. Mifsud, and E. D. Valentino, “Teleparallel gravity: from theory to cosmology,” *Reports on Progress in Physics*, vol. 86, no. 2, p. 026901, 2023.
- [32] G. Leon, K. F. Dialektopoulos, and A. Paliathanasis, “Cartan symmetries and global dynamical systems analysis in a higher-order modified teleparallel theory,” *General Relativity and Gravitation*, vol. 50, no. 79, 2018.
- [33] S. Nojiri and S. D. Odintsov, “Modified gravity with  $\ln r$  terms and cosmic acceleration,” *General Relativity and Gravitation*, vol. 36, pp. 1765–1780, 2004.
- [34] J. D. Barrow and S. Hervik, “Anisotropically inflating universes,” *Physical Review D—Particles, Fields, Gravitation, and Cosmology*, vol. 73, no. 2, p. 023007, 2006.